

## THE LARGE N EXPANSION IN THE STRONG CORRELATION PROBLEM

GABRIEL KOTLIAR

Serin Physics Laboratory, Rutgers University, Piscataway NJ  
08854 USA

### 1 Introduction

The recent discovery of exciting new materials like the heavy fermion systems and the cuprate high temperature superconductors has revived our interest in the strong correlation problem. That is the interplay between the localized and the itinerant character of d and f electrons in a crystal, a problem which has fascinated solid state physicists and chemists since the early 60's. We are interested in model hamiltonians which go under the name of extended Hubbard models or periodic Anderson lattices. The derivation of these hamiltonians and some of their basic properties are covered in the lectures by P. Littlewood in this school. The solutions of these models and the degree to which they describe the rich phenomena observed in the laboratory is still an open difficult problem. By its very nature, application of perturbation theory to this class of problems is not straightforward. One can diagonalize exactly the large local interaction terms in these hamiltonians, and attempt an expansion in the kinetic energy term. This term is formally small, but is a singular perturbation. On the other hand one can diagonalize exactly the kinetic energy and attempt an expansion in the much larger interaction terms. In this case there is no small parameter controlling the expansion, and the validity of this procedure is unclear.

At this point it is instructive to analyze toy models, that is study hamiltonians which can be solved exactly or systematically to try to gain useful

insights into the behaviour of more realistic models. This is one of the central theme of this school. There are several ways one can alter the models to make them simpler. One can modify the dimensionality, the symmetry group, and the representation of the symmetry group, to make the models simpler. One dimensional models are interesting in their own and have inspired ideas which can be generalized to finite dimensional systems. They have been covered in Emery's lecture in this school. The limit of infinite dimensionality offers drastic simplifications and an intriguing connection to  $0 + 1$  dimensional models. It is presently, the subject of intensive investigation. An introduction to this field is presented in D. Vollhardt's lectures in this school.

One can change the representation of the spin  $Su(2)$  group, from the fundamental two dimensional representation to higher (larger) representations and study the limit where the size of the representation goes to infinity. This is the semiclassical limit, covered in A. Auerbach's lectures. Alternatively one can modify the model by extending the spin  $SU(2)$  symmetry group to  $SU(N)$  where  $N$  is large. How this is done and what do we learn from the study of this generalization is the subject of these lectures. There are other ways to generalize the models we are interested in strong correlation physics, the symplectic group  $Sp(N)$ , reduces to  $Su(2)$  when  $N=1$  and the large  $N$ ,  $Sp(N)$  limit has been investigated[1] In these lectures we will not attempt to review the large literature of large  $N$  methods in many body theory. Our goal here is more modest, we will introduce the student to some of the concepts which may be useful for elucidating the strong correlation problem, and illustrate these concepts in models which become soluble as  $N$  gets large. Consequently the references to the literature is not exhaustive and we apologize in advance for possible omissions and for the somewhat biased, choice of topics.

In the first lecture we will illustrate the workings of the large  $N$  method in the context of a single spin interacting with conduction electrons and see how spins and conduction electrons can bind to form a scattering resonance. [2] [3] In the second lecture we present the large  $N$  solution of the extended Hubbard model. The large  $N$  limit serves as a laboratory in which we can study how changing the high energy parameters in the hamiltonian modifies the low energy physics. We focus here on the finite charge transfer energy aspect of this problem and show how the competition between charge transfer energy and hybridization gives rise to a metal insulator transition. [4] [5]. In

Table 1		
$ 0 \rangle$	$\longleftrightarrow$	$b^+ 0 \rangle$
$f_\sigma^+ 0 \rangle$	$\longleftrightarrow$	$\tilde{f}_\sigma^+ 0 \rangle$
$f_{phys\sigma}^+$	$\longleftrightarrow$	$f_\sigma^+b$
$\sum_\sigma f_{phys\sigma}^+ \leq 1$	$\longleftrightarrow$	$\sum_\sigma f_\sigma^+ f_\sigma + b^+b$

Table 1: Correspondence between the usual notation derived from the finite  $U$  hamiltonian and the slave boson notation which incorporates the  $U = \infty$  constraint

the third lecture we analyze the effects of the conduction electron bandwidth and relate the quasiparticle structures of the previous lecture with the Kondo resonances of the heavy fermion problem. [6] [7] [8] In the last lecture we discuss the effects of finite nearest neighbor repulsion. This term modifies the nature of the metal charge transfer insulator transition. In the conclusion we mention a few other topics which can be studied using the large  $N$  method and were not covered in these lectures, and outline some directions of further research beyond the large  $N$  limit.

## 2 The single impurity Anderson model

The first ingredient of many models is a strongly correlated level, that is a localized orbital where the on site repulsive interactions are so large that double occupancy is energetically forbidding. We will represent it using a slave boson - spin fermion decomposition. [9] [3]

When the orbital is empty we label it with a slave boson  $b^+|o \rangle$  when its occupied by a electron with spin  $\sigma$  we label it with  $f_\sigma^+|o \rangle$ . The exclusion of double occupancy is phrased as

$$\sum_\sigma f_\sigma^+ f_\sigma + b^+b = 1 \quad (1)$$

The local hamiltonian has the form

$$H_f = \epsilon_f^o \sum_\sigma f_\sigma^+ f_\sigma \quad (2)$$

This notation is summarized in table 1.

Table 2		
	$\sum_{\sigma} f_{\sigma}^{\dagger} f_{\sigma}$	$b^{\dagger} b$
$ 0\rangle$	0	1
$ \sigma\rangle$	1	0

Table 2: Fermi and bose occupation number in a local basis. the double occupancy constraint then becomes an equality constraint.

The states allowed by the constraint are shown schematically in table 2.

The introduction of the field  $b$  allows us to consider charge as well as spin fluctuations. If we take the limit  $\epsilon_f^o \rightarrow -\infty$ , the orbital is always singly occupied and we obtain a description of a localized spin degree of freedom.

At this point the introduction of  $b$  is a mathematical trick to transfer the double occupancy constraint into an equality constraint. Its significance and physical interpretation will emerge in the following lectures.

The infinite  $U$  single impurity Anderson model, describes the interaction of a correlated level with a band of delocalized electrons via a hybridization term. We generalize it from  $SU(2)$  to  $SU(N)$  by allowing the spin index to run from 1 to  $N$ , while we scale the hybridization as  $\frac{1}{\sqrt{N}}$ . The resulting hamiltonian is:

$$H = \sum_{\mathbf{K}\sigma} \epsilon_{\mathbf{K}} C_{\mathbf{K}\sigma}^{\dagger} C_{\mathbf{K}\sigma} + \sum_{\sigma} \epsilon_f^o f_{\sigma}^{\dagger} f_{\sigma} + \frac{V}{\sqrt{N}} \sum_{\mathbf{K}\sigma} C_{\mathbf{K}\sigma}^{\dagger} f_{\sigma} b^{\dagger} + f_{\sigma}^{\dagger} b C_{\mathbf{K}\sigma} \quad (3)$$

At the same time the original constraint is generalized to [3]

$$Q \equiv \sum_{\sigma} f_{\sigma}^{\dagger} f_{\sigma} + b^{\dagger} b = \frac{N}{2} \quad (4)$$

The physical electron operator which makes transitions between  $|o\rangle$  and  $|\sigma\rangle$  is described by  $f_{\sigma}^{\dagger} b$ . For  $N = 2$ ,  $f_{\sigma}^{\dagger} b b^{\dagger} f_{\sigma} = f_{\sigma}^{\dagger} f_{\sigma}$  when acting on states obeying the constraint (4).  $\sum_{\sigma} f_{\sigma}^{\dagger} f_{\sigma}$  is the correct generalization of the operator counting the number of  $f$  electrons for arbitrary  $N$ .

The partition function of the model described by Eqs. (3) and (4) is given by:

$$Z = \int df^{\dagger} df db^{\dagger} db d\lambda dC^{\dagger} dC e^{-S} \quad (5)$$

$$S = \int_0^\beta [b^\dagger \frac{\partial}{\partial \tau} b + \sum_{\mathbf{k}} C_{\mathbf{k}\sigma}^\dagger \frac{\partial}{\partial \tau} C_{\mathbf{k}\sigma} + i\lambda(Q - \frac{N}{2}) + f_\sigma^\dagger \frac{\partial}{\partial \tau} f_\sigma + H] d\tau \quad (6)$$

$\lambda$  is a lagrange multiplier which enforces the constraint. While it is clear that (5) (6) allows for a well defined large  $N$  limit it is not obvious whether the physics at large  $N$  is qualitatively the same as in the  $N=2$  case. In the single impurity case one can compare exact results and the results of the  $\frac{1}{N}$  approach and the agreement is excellent. [2] In more complicated problems comparison with other treatments is necessary to assess the reliability of the method.

The action possess a local gauge invariance, [2] i.e. upon a gauge transformation:

$$b(\tau) \rightarrow e^{i\theta(\tau)} b(\tau) \quad f(\tau) \rightarrow e^{i\theta(\tau)} f(\tau) \quad \lambda \rightarrow \lambda - \dot{\theta} \quad (7)$$

The action changes by a total derivative term. The physical electron creation operator  $f_\sigma^\dagger b$  is gauge invariant. The gauge symmetry is the formal manifestation of the constraint (4), which commutes with the hamiltonian. It is convenient to use this gauge invariance to work in radial gauge [2] where  $b$  and  $b^\dagger$  are real and denoted by  $r$ . The lagrange multiplier  $\lambda$  acts like a temporal component of a gauge field and absorbs the phase of the boson. This gauge is useful because the phase of  $f$  is the phase of the physical electron. This gauge is also free from infrared divergences. We will use it in section 4. The cartesian gauge [2] defined by the original lagrangian, has a time independent lagrange multiplier  $\lambda$  and a complex field  $b$ . It is better suited for treatment of the high energy behavior of the theory. We will illustrate its use in section 3.

The generalized model (3) (4) can be solved by the functional integral method introduced by Read and Newns [2]. Integrating out the conduction electrons one obtains an effective action for the bose fields

$$Z = \int db^\dagger db d\lambda e^{-N S_{eff}[b^\dagger, b, \lambda]} \quad (8)$$

When  $N$  is large one estimates  $Z$  by the saddle point method. The saddle point for the lagrange multiplier  $\lambda$  occurs along the imaginary axis  $i\lambda = \lambda_0$ , while the saddle point value of  $b$  is  $b = \sqrt{N} r_0$ . Substituting the saddle point values for  $b$  and  $\lambda$  in eq. (6) one obtains a saddle point lagrangian

$$L_{sp} = f_{\sigma}^{\dagger} \frac{\partial}{\partial \tau} f_{\sigma} + C_{k\sigma}^{\dagger} \frac{\partial}{\partial \tau} C_{k\sigma} + \sum_k \epsilon_k C_{k\sigma}^{\dagger} C_{k\sigma} + \epsilon_f f_{\sigma}^{\dagger} f_{\sigma} + V r_o \sum_k (C_{k\sigma}^{\dagger} f_{\sigma} + f_{\sigma}^{\dagger} C_{k\sigma}) \quad (9)$$

Eq. (9) describes non-interacting electrons in the presence of an impurity state with energy  $\epsilon_f = \epsilon_f^o + \lambda_o$  which hybridizes with a conduction band with a matrix element  $r_o V$ . This is the so called resonant level model. The large N saddle point hamiltonian gives a concrete realization of Fermi liquid ideas where simplicity is attained at low energies after a process of renormalization. In the Kondo case the fixed point hamiltonian is a resonant level model, and the large N method offers a concrete (but approximate) realization of this idea. The saddle point hamiltonian is (the large N version of) the fixed point hamiltonian which controls the low energy response functions and the low temperature thermodynamics.

At high temperatures and high energies the  $f^{\dagger}$  and the  $C^{\dagger}$  are essentially independent degrees of freedom. In the local moment limit we have free electrons and a free spin. At low temperature the excitonic correlation  $\langle \sum_k C_{\sigma k}^{\dagger} f_{\sigma} \rangle$  develops and the impurity spin is locked in a singlet with the conduction electrons. The effective degrees of freedom at low energies are fermionic quasiparticles and their lagrangian is given in eq. (9). Fluctuations of the bose field around the saddle point values generate effective interactions between quasiparticles. In terms of the saddle point lagrangian we can compute the  $f$  and conduction electron Green's functions. The transformation  $C_{k}^{\dagger}(\tau) \rightarrow C_{k}^{\dagger}(\tau) - \int d\tau' f^{\dagger}(\tau') r_o V G_o(\tau' - \tau)$  diagonalizes the lagrangian and allows to evaluate the mean field Greens functions:

$$\begin{aligned} - \langle f f^{\dagger} \rangle_{sp} &= \frac{1}{i\omega_n - \epsilon_f - G_o^o(i\omega_n) r_o^2 V^2} = G_{ff}(i\omega_n) \\ - \langle f C_K^{\dagger} \rangle_{sp} &= \frac{1}{(i\omega_n - \epsilon_K)} V r_o G_{ff} = G_{fK}(i\omega_n) \quad (10) \\ - \langle C_K C_{K'}^{\dagger} \rangle_{sp} &= \frac{\delta_{KK'}}{(i\omega_r - \epsilon_K)} + r_o^2 V^2 \frac{1}{(i\omega_r - \epsilon_K)} G_{ff}(i\omega_n) \frac{1}{(i\omega_r - \epsilon_{K'})} \end{aligned}$$

Here we introduce the conduction electron Greens functions  $G_o(k, i\omega_n) = \frac{1}{(i\omega_n - \epsilon_k)}$  and  $G_o^o(i\omega_n) = \sum_K \frac{1}{(i\omega_n - \epsilon_k)}$ . The conduction electron density of states

$\rho(\epsilon) = \frac{1}{V} \sum_{\mathbf{k}} \delta(\epsilon - \epsilon_{\mathbf{k}})$ . Eq. (10) shows that in the large  $N$  limit,  $G_{ff} V^2 r_o^2$  is the  $t$  matrix of the conduction electrons. Notice that  $G_{ff}$  is not the physical electron Green's function (which will be defined below), but the Greens function of the quasiparticle in the large  $N$  limit.

The saddle point conditions which determine the value of  $\lambda_o$  and  $r_o$  are obtained by differentiating the effective action (7) with respect to  $r_o$  and  $\lambda_o$ . The equations obtained can be expressed in terms of the mean field hamiltonian as

$$r_o^2 N + \sum_{\sigma n} \langle f_{\sigma}^+ f_{\sigma} \rangle_{sp} e^{i\omega_n \tau_o^+} = \frac{N}{2} \quad (11)$$

$$-\lambda_o r_o = \frac{r_o V}{N} \sum_{K \sigma_n} \langle f_{\sigma}^+ C_{K\sigma} \rangle_{sp} e^{i\omega_n \tau_o^+} \quad (12)$$

Here  $\langle . \rangle_{sp}$  denotes an expectation value in the thermal state determined by the saddle point hamiltonian. This form of the saddle point equations exhibits the mean field, self consistent character of the theory. We can rewrite them in terms of the saddle point Green's functions of eq. 10, and the Fermi Dirac distribution function  $f(y)$

$$-\int_{-\infty}^{\infty} \frac{dy}{\pi} f(y) \text{Im} G_{ff}(y) = \frac{1}{2} - r_o^2 \quad (13)$$

$$\lambda_o r_o = \int_{-\infty}^{\infty} \frac{dy}{\pi} f(y) \text{Im} [G_o G_{ff}] V^2 r_o \quad (14)$$

To analyze these equations we take the zero temperature,  $T = 0$ , limit and use a model density of states  $\rho(\epsilon) = \frac{2}{\pi W^2} \sqrt{W^2 - \epsilon^2}$  to evaluate the momentum summations.  $W$  is the conduction electron bandwidth. It is instructive to analyze the local moment regime limit of these equations.  $\epsilon_f^0 \rightarrow -\infty$ ,  $V \rightarrow \infty$  with  $J = \frac{V^2}{\epsilon_f^0}$  finite. In this limit  $r_o \rightarrow 0$  while  $(V r_o)^2 \rho_f \pi \equiv \Delta$  and  $\epsilon_f$  remain finite,  $\rho_f \equiv \rho(\epsilon_f)$ .

If we assume that the conduction band is half filled so as to have a particle hole symmetric situation, the first equation forces  $\epsilon_f = 0$ . The second equation then determines  $\Delta$ . To analyze the qualitative behavior of the solution we approximate the Green's function

$$G_o^{-1}(x) = \frac{x + \sqrt{x^2 - W^2}}{2} \simeq \frac{iW}{2} \quad x \ll W \quad (15)$$

$$\simeq x \quad x \gg W \quad (16)$$

In the weak coupling limit (i.e.  $\rho J \ll 1$ ) eq. (14) reduces to  $\frac{1}{\gamma} = \rho_f \log \frac{\Delta}{W}$ .  $\Delta = W \exp - (\frac{1}{\rho J})$  is a nonperturbative expression in the coupling  $\frac{J}{W}$  it sets the Kondo scale  $T_K$  at which the spin and conduction electrons bind. [2]

In the limit that the bandwidth is small ( $J \gg W$ ) a new feature appears [10] [11]: the real part of the  $f$  self energy is no longer negligible and true bound states are formed below the bottom of the band.  $G_{ff} = \frac{1}{x - \frac{1}{2}\Delta}$  for  $x \gg W$  and a new pole appears at  $x \approx \sqrt{\frac{\Delta W}{2}} \gg W$ . In this case (14) is dominated by the contribution from this pole and we find  $\sqrt{\frac{W\Delta}{2}} \approx \frac{J}{2}$ . This is the Nozieres strong coupling limit in which a resonance is pulled out outside the band. The crossover from weak coupling to strong coupling is smooth. The appearance of bound states outside the band does not imply any discontinuity in the low energy properties of the system.

The low temperature thermodynamics is determined from the quasiparticle hamiltonian. This is a resonant level model, the spin degrees of freedom have been transmuted into a spinless resonance and spin  $\frac{1}{2}$   $f$ -quasiparticles. The expressions for  $\chi$  and  $C_V$  are (to leading order in  $\frac{1}{N}$ ) those of a resonant level model i.e.

$\chi \sim \gamma \sim \delta'(0)$  The phase shift  $\delta$  is obtained as the argument of the  $t$  matrix:

$$\delta(x) = \arctg\left(\frac{\Delta(x)}{\epsilon_f + \Sigma(x) - x}\right) \quad (17)$$

Here  $\Delta(x) = -V^2 r_o^2 \text{Im} G_o^>$  and  $\Sigma(x) = -V^2 r_o^2 \text{Re} G_o^>(x)$ . Inserting the solution of the mean field equations in (17) we find that in the weak coupling limit  $\chi \sim \gamma \sim \frac{1}{T_K}$ , and  $\frac{\chi}{\gamma} = 1$ . The density of states of the quasiparticles is strongly enhanced ( $T_K \ll W$ ), the result of the large spin susceptibility and entropy of a spin degree of freedom which has been transferred to the quasiparticles. In the strong coupling limit  $\Delta \gg W$  and the renormalizations are very small and negative. [11].

The next order  $\frac{1}{N}$  corrections are obtained by studying the fluctuations of the Bose fields around their saddle point values. They can be thought of as describing the effective interactions between the quasiparticles which bring additional renormalizations to  $\chi$  and  $C_V$ . They increase the Wilson ratio from the non interacting quasiparticle value towards the exact result  $\frac{\chi}{\gamma} = 2$  at  $N=2$  in the weak coupling limit. An important feature of the slave boson technique

should be noticed at this point. The f spectral function is concentrated at energies within  $T_K$  of the Fermi level. Of course one would expect that most of the spectral weight of the f electrons is at high energy around the bare f level  $\epsilon_f^0$ . This part of the spectral weight is recovered by computing the physical f electron correlation function  $-\langle f(\tau)b^+(\tau)b(o)f^+(o) \rangle$  to order  $\frac{1}{N}$ . [3] We will not do this here but we will illustrate how the fluctuations of the Bose fields generate the incoherent part of the spectral function in the section on the extended Hubbard model.

### 3 The Extended Hubbard Model: The Metal Charge Transfer Insulator Transition

The infinite  $U$  three band extended Hubbard model describes the two configurations,  $Cu^{++}$  and  $Cu^+$  on the copper atoms denoted by  $d_\sigma^+|0\rangle$  and  $|0\rangle$  respectively, and oxygen holes in  $\sigma$  orbitals along the x and y axis denoted  $p_{x\sigma}^+|0\rangle > p_{y\sigma}^+|0\rangle$ . The "vacuum"  $|0\rangle$  is taken to be the closed shell configuration  $Cu^+O^{--}$ . The quantum chemistry of this Hamiltonian for high  $T_c$  and heavy fermions systems is described in P. Littlewood lectures in this school. Here we will be concerned with its generalization from  $SU(2)$  to  $SU(N)$  which is given by

$$\begin{aligned}
H = & \sum_{i\sigma} d_{i\sigma}^+ d_{i\sigma} \epsilon_d^0 + \sum_{i\sigma\alpha=x,y} \epsilon_p^0 p_{i\sigma\alpha}^+ p_{i\sigma\alpha} - t_p \sum_K [p_{kx\sigma}^+ p_{kx\sigma} 4 \sin \frac{k_x}{2} \sin \frac{k_y}{2} + c.c] \\
& - \frac{t_{pd}}{\sqrt{N}} \sum_{i\sigma} [(p_{ix\sigma}^+ - p_{i\sigma-x}^+ + p_{iy\sigma}^+ - p_{i\sigma-y}^+) d_{i\sigma} b_i^+ + h.c] \\
& + \frac{J}{N} \sum_{(ij)\sigma\sigma'} d_{i\sigma}^+ d_{i\sigma'} d_{j\sigma'}^+ d_{j\sigma} \\
& + \frac{V}{N} \sum_{i\sigma\sigma'} d_{i\sigma}^+ d_{i\sigma} \sum_{\alpha=\pm x \pm y} (p_{i\sigma'\alpha}^+ p_{i\sigma\alpha}) \\
& + \frac{V_2}{N} \sum_{i\sigma\sigma'} d_{i\sigma}^+ d_{i\sigma'} \sum_{\alpha=\pm x \pm y} p_{i\sigma'\alpha}^+ p_{i\sigma\alpha} \tag{18}
\end{aligned}$$

As discussed in the previous section the local constraints excluding the  $Cu^{+++}$  state is generalized to

$$Q_i \equiv \sum_{\sigma} d_{i\sigma}^{\dagger} d_{i\sigma} + b_i^{\dagger} b_i = \frac{N}{2} \quad (19)$$

The introduction of the copper copper superexchange  $J$  as a new term in the Hamiltonian requires some justification. This allow us to treat effects of the copper copper superexchange at the  $N = \infty$  order. If not included in the bare hamiltonian, a term of this form would be generated in  $\frac{1}{N^2}$  order [12], and therefore it is important to included it in the action from the very beginning . The superexchange has its origin in is virtual, high energy processes and one can imagine integrating those to generate the term proportional to  $J$  in eq. (18), and then treat lower energy phenomena using the large  $N$  expansion. In order not to double count diagrams, the loop integrals should be done with a reduced upper cutoff. The validity of this approach was tested in the study of the two impurity Kondo problem, where this approach can be tested against exact renormalization group results. [13] For some reference on the effects of this term within the large  $N$  framework see [38] [39].

The term  $V$  is the nearest neighbor repulsion proposed by Varma et al. [14] as the origin of the pairing mechanism in these systems.  $V_2$  describes the exchange effects of the nearest neighbor repulsion and should be taken to be  $\frac{V}{2}$  so as to reproduce the Hartree and the exchange graphs when  $N = 2$ . This term can be also interpreted as an additional Kondo exchange between copper and oxygen which is unrelated to the pd hybridization. Density functional and empirical fits to various photoemission spectra calculations give [15]

$$\frac{t_{pd}}{\sqrt{2}} = 1.3, \epsilon_p^o - \epsilon_d^o = 3.6, V = 1.2, J \simeq .13, t_p \equiv .6$$

The large  $N$  framework has been used to calculate the optical conductivity, the one particle spectral function and various other response functions in a set up which includes a realistic band structure and non perturbative renormalizations due to correlations. For a partial guide to the literature the reader is referred to [18] [8] [16] [17]. It is worthwhile to stress again, that one can view the large  $N$  approach as an explicit, non perturbative, construction of the quasiparticle hamiltonian corresponding to the bare hamiltonian (18) and the mean field equations allows us to understand how changing the various (high energy) couplings in the Hamiltonian (18) affects the quasiparticle

(low energy) parameters. The fluctuation of the Bose fields then regenerate the incoherent parts of the spectral functions and give rise to the residual interactions among the quasiparticles. The large  $N$  expansion to next to leading order in  $\frac{1}{N}$ , then provides a framework to analyze the itinerant and localized aspects of the excitations, the coherent and the incoherent features of the one particle spectrum and the possible instabilities of the Fermi liquid.

In this lecture we will analyze in some detail the simplest limit of this model. We will take  $V = V_2 = 0, t_p = 0, J = 0$ . We shall see that even this simple “bare bones” charge transfer model contains the essential ingredients necessary to produce a metal-charge transfer insulator transition. A thorough understanding of this simple model is necessary to appreciate the qualitative differences brought about by the various other interactions.

The starting point of our analysis of the extended three-band Hubbard model with  $SU(2)$  spin generalized to  $SU(N)$  flavors [4] is the expression of the partition function as a coherent state path integral:

$$Z = \int \prod_i db_i^\dagger db_i d\lambda_i \prod_{\alpha=x,y\sigma} dp_{i\alpha\sigma}^\dagger p_{i\alpha\sigma} \prod_{\sigma} dd_{i\sigma}^\dagger dd_{i\sigma} e^{-\int_0^\beta L} \quad (20)$$

with a lagrangian  $L$  given by:

$$\mathcal{L} = \sum_{i,\sigma} d_{i\sigma}^\dagger (\partial/\partial\tau + \epsilon) d_{i\sigma} + \sum_{i,\alpha,\sigma} p_{i\alpha\sigma}^\dagger (\partial/\partial\tau + \epsilon) p_{i\alpha\sigma} + \sum_i b_i^\dagger \partial/\partial\tau b_i + \quad (21)$$

$$- \frac{t_{pd}}{\sqrt{N}} \sum_{i,\eta,\sigma} \text{sgn}(\eta) (p_{i\eta\sigma}^\dagger d_{i\sigma} b_i^\dagger + h.c.) + i \sum_i \lambda_i (\sum_{\sigma} d_{i\sigma}^\dagger d_{i\sigma} + b_i^\dagger b_i - N/2)$$

where  $\alpha = x, y$  and  $\eta = \pm x, \pm y$ , and  $\lambda_i$  is a Lagrange multiplier enforcing the infinite- $U_d$  constraint on the copper site. Its main role is to shift the bare copper level.  $b_i$  is a slave boson whose expectation value renormalizes the coherent hybridization between the copper  $3d_{x^2-y^2}$  orbitals ( $d_{\sigma}^\dagger$ ) and the oxygen  $2p_x$  and  $2p_y$  orbitals ( $p_{x\sigma}, p_{y\sigma}$ ). We then have a theory of fermions interacting with two bose fields,  $\lambda$  and  $b$ . There are two parameters in the problem the doping  $\delta$  and the ratio of hybridization to charge transfer energy  $\frac{t_{pd}}{E}$ ,  $E \equiv \epsilon_p - \epsilon_d^0$ . At  $\delta = 0$  we expect the physics to be very different depending on whether  $t_{pd} \gg E$  or  $t_{pd} \ll E$ . In the latter case it is reasonable to start with a ground state with each copper singly occupied. The copper

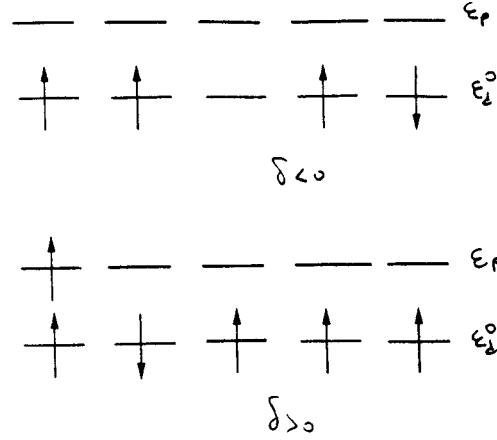


Figure 1: A caricature of the occupation of the energy levels in copper oxide lattice in the  $t_{pd} \ll E$  limit for  $\delta < 0$  (electron doped case) (fig a) and  $\delta > 0$  (hole doping) fig b.

does not hybridize with the oxygen since in order to hybridize we need to promote a hole from copper to oxygen ( and therefore pay a charge transfer energy  $E$ ) while the hybridization (i.e. the delocalization energy gained by being able to move around) is only  $\frac{t_{pd}^2}{E}$ . We then have a charge transfer insulator at half filling. If we dope with holes  $\delta > 0$  we add a hole on the oxygen site, and the chemical potential  $\mu \approx \epsilon_p$ . If we dope with electrons ( $\delta < 0$ ) we remove a hole on the copper site, and the chemical potential  $\mu \approx \epsilon_d^0$ . See fig (1).

If  $t_{pd} > E$  we have a very different state of affairs. It pays to promote holes from copper to oxygen since the gain in hybridization is very large. We have a strong mixture of copper and oxygen at low energies and we generate a metallic state. At half filling we expect a metal insulator transition as a function of  $E$ . For large  $E$  the chemical potential jump at half filling,  $\Delta\mu$  is given by  $\epsilon_p - \epsilon_d^0$ . Increasing  $t_{pd}$  reduces  $\Delta\mu$  until it vanishes at the metal insulator transition.

These expectations are borne out by the  $N = \infty$  limit of the model

When  $N \rightarrow \infty$  the path integral is controlled by its saddle point value.  $Z \simeq e^{-N_S N \beta S_{SP}}$  where the uniform saddle point action  $S_{SP}$  is given:

$$S_{sp} = \lambda(r_o^2 - \frac{1}{2}) - \frac{1}{3} \sum_{K\alpha} \ln(1 + e^{-\beta E_{\alpha h}}) \quad (22)$$

and  $E_{\mathbf{k}}$  are the eigenvalues of the 3x3 matrix  $H_{\mathbf{k}}$

$$H_{\mathbf{k}} = \begin{bmatrix} \epsilon_p & & 2\gamma_{\mathbf{k}} S_x(r_o t_{pd}) \\ & \epsilon_p & 2\gamma_{\mathbf{k}} S_y(r_o t_{pd}) \\ 2\gamma_{\mathbf{k}} S_x(r_o t_{pd}) & 2\gamma_{\mathbf{k}} S_y(r_o t_{pd}) & \epsilon_d \end{bmatrix} \quad (23)$$

with  $S_{\alpha} = \sin \frac{k_{\alpha}}{2}$ ,  $\alpha = x, y$  and  $\gamma_{\mathbf{k}}^2 = S_x^2 + S_y^2$ . Here we have introduced the notation  $\epsilon_d = \epsilon_d^o + \lambda_o$  for the renormalized d level. We define the Fourier transform of the operators d and p :

$$d_{\mathbf{i}} = \frac{1}{\sqrt{N_s}} \sum_{\mathbf{k}n} e^{i(\mathbf{k}R_{\mathbf{i}} - \omega_n \tau)} d_{\mathbf{k}\sigma}$$

$$p_{\mathbf{i}\alpha\sigma} = \frac{1}{\sqrt{N_s}} \sum_{\mathbf{k}n} e^{i(\mathbf{k}R_{\mathbf{i}} - \omega_n \tau)} p_{\mathbf{k}\alpha\sigma} e^{i\mathbf{k} \cdot \frac{2\mathbf{a}}{3}}$$

$e_{\alpha}$  is a lattice unit vector  $\alpha = \pm x \pm y$ .

It is useful to introduce a unitary matrix U which diagonalizes the saddle point lagrangian  $L_{\infty}$ . It defines a canonical transformation ( $\Phi_{\mathbf{k}\sigma,l} = \sum_{l'} U_{l,l'}(\mathbf{k}) \Psi_{\mathbf{k}\sigma,l'}$ ) from the copper oxygen orbitals  $\Psi_{\mathbf{k}\sigma,l} = (d_{\mathbf{k}\sigma}, ip_{\mathbf{k}\sigma,x}, ip_{\mathbf{k}\sigma,y})$  to the quasiparticle basis  $\Phi_{\mathbf{k}\sigma,l} = (c_{\mathbf{k}\sigma 1}, c_{\mathbf{k}\sigma 2}, c_{\mathbf{k}\sigma 3})$ .

$$U(\mathbf{k}) = \begin{pmatrix} u_{\mathbf{k}} & s_x v_{\mathbf{k}} & s_y v_{\mathbf{k}} \\ v_{\mathbf{k}} & -s_x u_{\mathbf{k}} & -s_y u_{\mathbf{k}} \\ 0 & s_y & -s_x \end{pmatrix}. \quad (24)$$

In the quasiparticle basis the saddle point lagrangian is diagonal

$$\mathcal{L}_{\infty} = \sum_{\mathbf{k}\sigma, l_n} \Phi_{\mathbf{k}\sigma l}^{\dagger}(\nu_n) (i\nu_n - E_l(\mathbf{k})) \Phi_{\mathbf{k}\sigma l}(\nu_n) \quad (25)$$

The eigenvalues  $E_i$  give the dispersions of the quasiparticle bands (bonding antibonding and nonbonding respectively).

$$E_1 = \frac{\epsilon_p + \epsilon_d - R}{2}$$

$$E_2 = \frac{\epsilon_p + \epsilon_d + R}{2}$$

$$E_3 = \epsilon_p$$

$$R_K \equiv \sqrt{(\epsilon_p - \epsilon_d)^2 + [4\gamma_{\mathbf{k}}(r_o t_{pd})]^2} \quad (26)$$

An important parameter is the energy difference between the  $\Delta \equiv \epsilon_p - \epsilon_d$  renormalized p and d levels. Straightforward differentiation of the saddle point action (22) give the mean field equations:

$$r_0^2 + \frac{1}{N_s} \sum_{\mathbf{k}} u_{\mathbf{k}}^2 f_1 + v_{\mathbf{k}}^2 f_2 = \frac{1}{2} \quad (27)$$

$$\lambda_0 = \sum_{\mathbf{k}} \frac{4\gamma_{\mathbf{k}}^2 t_{pd}^2}{R_{\mathbf{k}}} (f_1 - f_2) \quad (28)$$

$$(29)$$

The doping  $\delta$  fixe the chemical potential via

$$\frac{1}{N_s} \sum_{\mathbf{k}} f_{1\mathbf{k}} + f_{2\mathbf{k}} + f_{3\mathbf{k}} = \frac{(1 + \delta)}{2}$$

The renormalized atomic level difference is  $\epsilon \simeq \epsilon_p - \epsilon_d = \epsilon_p - \epsilon_d^0 - \lambda_0$ . The Bogolubov coefficients are  $u_{\mathbf{k}}^2 = (1 + \epsilon/R_{\mathbf{k}})/2$ , and  $v_{\mathbf{k}}^2 = (1 - \epsilon/R_{\mathbf{k}})/2$ .  $N_s$  is the number of unit cells and  $f_{i\mathbf{k}} = f(E_i(\mathbf{k}) - \mu)$  are the Fermi distribution functions.

The mean field equations (27) - (29) can be analyzed to conclude that a second order Brinkman-Rice transition takes place at  $\delta = 0$  at a critical value of the charge transfer gap  $E_c = (\epsilon_p - \epsilon_d^0)_c = 4t_{pd}(\overline{\gamma_{\mathbf{k}}^2})^{1/2}$  where  $\lambda_0^c = \Delta_c = 2t_{pd}(\overline{\gamma_{\mathbf{k}}^2})^{1/2}$  and  $\overline{\gamma_{\mathbf{k}}^2} = \frac{1}{N_s} \sum_{\mathbf{k}} \gamma_{\mathbf{k}}^2 f_{1\mathbf{k}} = 1/2 + 2/\pi^2$ . As we approach the critical point the coherence parameter  $r_0^2$  vanishes according to  $r_0^2 = \frac{1}{6} [(\overline{\gamma_{\mathbf{k}}^2})^{3/2}/\overline{\gamma_{\mathbf{k}}^4}] (E_c - E)/t_{pd}$ . Here  $\overline{\gamma_{\mathbf{k}}^4} \equiv \frac{1}{N_s} \sum_{\mathbf{k}} \gamma_{\mathbf{k}}^4 f_{1\mathbf{k}} = 5/8 + 4/\pi^2$ .

These results allows us to determine the behavior of the quasiparticle weight  $Z_{QP}$ , the effective mass and the magnetic susceptibility as we approach the metal charge transfer insulator transition from below. Our results are identical to those obtained for the Hubbard model by Brinkman and Rice if we identify the Hubbard  $U$  with the bare charge transfer energy  $E$ .

$$\frac{m}{m^*} \simeq Z_{QP} \simeq \chi^{-1} \simeq (E_c - E) \quad (30)$$

At this stage magnetic effects have not been introduced in our calculation. Including the superexchange explicitly in the  $N = \infty$  theory will modify the relation between the effective mass and the quasiparticle residue. These and

various other low energy manifestations of the superexchange in the large N framework are discussed in refs. [8] [37].

At the critical point the renormalized d level lies exactly in the middle of the charge transfer gap, i.e.  $\epsilon = \frac{E_c}{2}$  at  $E = E_c = 4t_{pd}(\gamma_k^2)^{1/2}$ . The effective d level has a singular correction near this point:

$$\epsilon \sim \frac{E_c}{2} - \frac{1}{2} \sqrt{|E - E_c| 2E_c} \quad (31)$$

It is important to emphasize that, on the insulating side ( $E > E_c$ ), the chemical potential jumps discontinuously as one goes from hole to electron doping  $\Delta\mu = \lambda_0(\delta = 0^+) - \lambda_0(\delta = 0^-)$ . This jump is affected by the singular shift of the d level and it vanishes as:

$$\Delta\mu = \sqrt{E^2 - 16t_{pd}^2\gamma_k^2} = |\lambda_0 - \Delta| \propto (E - E_c)^{\frac{1}{2}} \quad (32)$$

as we approach  $E_c$  from above. The compressibility vanishes as we approach the critical point, at half filling from the metallic side [22]

$$\frac{\partial n}{\partial \mu} \propto (E - E_c) \quad (33)$$

For  $\delta = 0$  and  $E > E_c$ ,  $\frac{\partial n}{\partial \mu} = 0$ . But the compressibility at an infinitesimally small doping is finite, and it vanishes as E is reduced towards the critical point.[21]

$$\frac{\partial n}{\partial \mu}(\delta = 0^+) \approx \sqrt{E - E_c} \quad (34)$$

Doping the charge transfer insulator gives rise to renormalized quasiparticle bands. Their dispersion is given by eqs. (26) and simplifies in the limit that  $E \gg E_c$ .

$$E_k^1 = \epsilon_p - \frac{E_c^2}{4E} - \delta \frac{E_c^2}{8E} \gamma_k^2 / \gamma_k^2 \quad \delta > 0 \quad (35)$$

$$E_k^1 = \epsilon_{d0} + \frac{E_c^2}{4E} + \delta \frac{E_c^2}{8E} \gamma_k^2 / \gamma_k^2 \quad \delta < 0 \quad (36)$$

these quasiparticles obey Luttinger theorem and their effective bandwidth is proportional to the number of holes. Notice that for  $\delta > 0$  the effective d level is pulled below the p level by an amount  $\frac{E_c^2}{E}$  which can be interpreted as the hybridization energy gained by an oxygen hole. [23]

The large N limit of the extended Hubbard model, then provides an example of a Mott transition in a soluble model. This is a metal insulator transition driven by correlations without the intervention of magnetic long range order. This occurs because the large N limit suppresses the magnetism, unless J is included explicitly in the formalism. The fate of this transition with finite J is discussed in ref [21]. The finite exchange modifies the connection between the quasiparticle residue  $Z_{QP}$  and the effective mass or the magnetic susceptibility [22] [21] as in the t-J model in the large N limit. [38] For instance:

$$\chi^{-1} \approx \frac{\alpha J + \delta t_{pd}^2}{(\epsilon_p - \epsilon_d^0)} \quad Z_{QP} \approx \delta \left[ \frac{t_{pd}}{(\epsilon_p - \epsilon_d^0)} \right]^2 \quad (37)$$

$\alpha$  is a finite constant which makes the susceptibility finite at the metal insulator transition. The statement that above the metal charge transfer insulator transition there is no hybridization between copper and oxygen is a slight oversimplification. A more accurate statement is that there is no coherent hybridization at low energies between the copper and the oxygen operators. We will see that at finite frequencies there is always hybridization (by an amount proportional to  $\frac{t_{pd}^2}{E}$ ) in the incoherent part of the one particle Green's function.

Now we would like to discuss this transition from the point of view of the Bose degrees of freedom. This picture, which is dual to the fermionic picture, illuminates a different aspect of the Mott phenomenon. To this end, we focus on the limit of half filling with  $\delta \rightarrow 0^\pm$ . We also focus on the "high frequency" limit  $\omega \gg \delta t$  which allows to ignore the Bose condensation. The action for the Bose degrees of freedom is obtained by integrating out the  $p$  and  $d$  fermion excitations from  $\mathcal{L}$ . It has a very simple form in Cartesian gauge. Denote  $(\bar{b}, \bar{b}^\dagger) \equiv (b, b^\dagger)/\sqrt{N}$ , then

$$\mathcal{L}_b = N \sum_{\vec{q}, \omega_n} \bar{b}^\dagger(\vec{q}, i\omega_n) [-i\omega_n + \lambda_0 - \Pi_{pd}(\vec{q}, i\omega_n)] \bar{b}(\vec{q}, i\omega_n), \quad (38)$$

where  $\Pi_{pd}$  is the usual interband polarization bubble,  $\Pi_{pd}(\vec{q}, i\omega_n) = 4t_{pd}^2 \gamma_{\vec{k}+\vec{q}}^2 / (i\omega_n + \Delta)$ ,  $\Delta \equiv \epsilon_p - \epsilon_d$ ,  $\gamma_{\vec{k}+\vec{q}}^2 = \frac{1}{N_s} \sum_{\mathbf{k}} \gamma_{\mathbf{k}+\mathbf{q}}^2 f_{1\mathbf{k}}$ . We obtain the Bose field propagator

$$(\bar{b}(\vec{q}, i\omega) \bar{b}^\dagger(\vec{q}, i\omega)) = \frac{Z_{\vec{q}}^s}{i\omega_n - \omega_{\vec{q}}^s} + \frac{Z_{\vec{q}}^e}{i\omega_n - \omega_{\vec{q}}^e}, \quad (39)$$

with  $Z_{\vec{q}}^{\alpha} = -(\omega_{\vec{q}}^{\alpha} + \Delta)/(\omega_{\vec{q}}^{\alpha} - \omega_{\vec{q}}^{\beta})$ ,  $\alpha \neq \beta = s, e$ . The poles in the propagator (39) defines two collective modes  $\omega^s$  and  $\omega^e$  corresponding to holon and charge transfer exciton respectively. The general dispersion of the modes is given by

$$\omega_{\vec{q}}^{1,2} = \frac{1}{2}(\lambda_0 - \Delta) \pm \frac{1}{2}\sqrt{(\lambda_0 - \Delta)^2 + 4\lambda_0\Delta\Omega(\vec{q})}, \quad (40)$$

which simplifies in the large charge transfer gap limit into

$$\omega_{\vec{q}}^s = -\frac{\lambda_0\Delta}{\lambda_0 - \Delta}\Omega(\vec{q}); \quad \omega_{\vec{q}}^e = \lambda_0 - \Delta + \frac{\lambda_0\Delta}{\lambda_0 - \Delta}\Omega(\vec{q}) \quad (41)$$

and  $\Omega(\vec{q}) = 1 - \frac{\gamma_{\vec{k}+\vec{q}}^2}{\gamma_{\vec{k}}^2} = \frac{2}{\pi^2} \frac{\gamma_{\vec{q}}}{\gamma_{\vec{k}}^2} \propto q^2$  for small  $\vec{q}$ . Therefore, in the hole doped case ( $\delta \rightarrow 0^+$ ),  $\omega_{\vec{q}}^s < 0$  and  $\omega_{\vec{q}}^e > 0$ , whereas this situation is reversed for electron doping ( $\delta \rightarrow 0^-$ ) where  $\omega_{\vec{q}}^s > 0$  and  $\omega_{\vec{q}}^e < 0$ . Note that for  $\delta > 0$   $\lambda_0 \sim \epsilon_p - \epsilon_d^e - \frac{t^2}{E}$  and  $\Delta = \epsilon_p - \epsilon_d$  is small. The opposite is true when  $\delta < 0$  which makes the particle-hole symmetry of this transition manifest. In either case, the modes disperse over a characteristic energy scale  $t \equiv t_{pd}^2/(\epsilon_p - \epsilon_d^e)$ , which are displayed in Fig. (2).

Expressions (32) and (41) establish that the energy of the charge transfer exciton is identical to the jump in the chemical potential as one goes from hole to electron doping:  $\Delta\mu = \omega_{\vec{q}=0}^e$ .

At finite doping  $r_0 \neq 0$ , it is convenient to work in the radial gauge to avoid the unphysical infrared divergence by writing  $b_i = \sqrt{N}r_0(1 + r_i)e^{i\theta_i}$  and absorbing the phase  $\theta_i$  into the Lagrange multiplier  $i\lambda_i = \lambda_0 + i\lambda_i + i\partial_{\tau}\theta_i$  [2]. The action governing the leading  $1/N$ -fluctuations is then, after integrating out the fermionic quasiparticles  $\Phi_i$ ,  $\mathcal{L}_{\mathbf{b}} = 2r_0^2 N \sum_{\vec{q}, \omega} A(\vec{q}, \omega) D^{-1}(\vec{q}, \omega) A(-\vec{q}, -\omega)$  with  $D$  the propagators of the Bose field  $A = (r, \lambda)$ . In the insulating phase ( $E > E_c$ ), we find

$$2D^{-1}(\vec{q}, \omega) = \begin{bmatrix} \lambda_0 - \frac{\lambda_0\Delta^2}{\Delta^2 - \omega^2}(1 - \Omega(\vec{q})) & i(1 - \frac{\lambda_0\Delta}{\Delta^2 - \omega^2})(1 - \Omega(\vec{q})) \\ i(1 - \frac{\lambda_0\Delta}{\Delta^2 - \omega^2})(1 - \Omega(\vec{q})) & \frac{\lambda_0}{\Delta^2 - \omega^2}(1 - \Omega(\vec{q})) - \frac{\lambda_0}{\omega^2}\Omega(\vec{q}) \end{bmatrix} \quad (42)$$

where we have retained only the leading terms in the zero doping limit. The dispersions of the collective modes are determined by the poles in the Bose propagators. Solving  $\det D^{-1}(\vec{q}, \omega_{\vec{q}}) = 0$  leads to  $\omega_{\vec{q}} = \pm\omega_{\vec{q}}^{1,2}$  in agreement with Eq.(40). At moderate hole concentration, the system forms a neutral

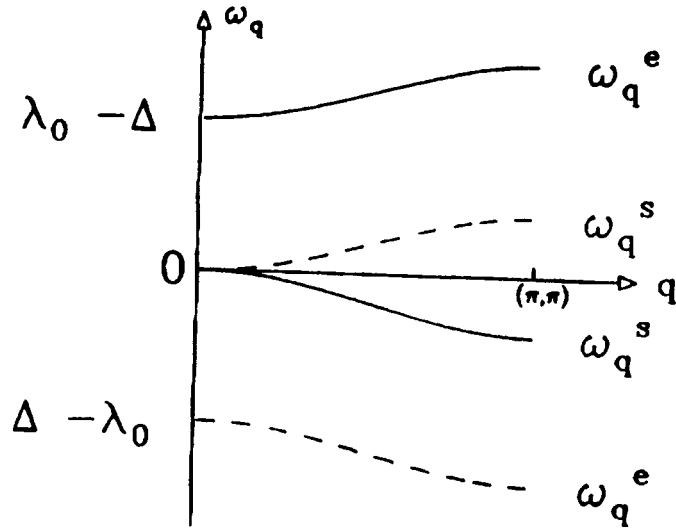


Figure 2: An illustration of the dispersion of the holon and exciton modes in the insulating limit. Solid line:  $\delta \rightarrow 0^+$ . Dashed line:  $\delta \rightarrow 0^-$ .

Fermi liquid and the holon mode smoothly crosses over to the usual (linearly dispersing) zero sound mode in the long wavelength limit [40], which shows up in  $\omega_q^s$  had we kept the next to leading order in  $r_0^2$  contributions in the matrix (42).

At small but *finite* doping, the modes  $\omega_q^{s,e}$  appear as poles (which turn into resonances when we include damping effects of order  $\frac{1}{N^2}$ ) in the density-density and stress-stress correlation functions, identifying themselves with the collective modes of the strongly correlated metal. However, near half-filling, for  $E > E_c$ , these collective modes have a vanishing ( $\approx r_0^2$ ) spectral weight, as direct excitations in the response functions, to next to leading order in  $\frac{1}{N}$ .

At this point the modes appear as poles in the Bose propagators which are auxiliary quantities. Physical quantities are obtained as convolutions of these entities with fermionic or other bosonic excitations in complete analogy with the one dimensional construction of physical excitations in terms of holons and spinons [31]. To relate these modes to observables we compute the optical absorption in the insulating limit. The current operator is given by ( $e = \hbar = 1$ ).  $J_{i,\alpha} = i(t_{pd}/2) [d_{i\sigma}^\dagger b_i(p_{i+\alpha/2,\sigma} + p_{i-\alpha/2,\sigma}) - c.c.]$ . The opti-

cal conductivity is determined by the imaginary part of the current-current correlator  $\Pi_{\mathbf{J}}(\vec{q}, \tau) = -\langle T_{\tau} J_{\mathbf{x}}^{\dagger}(\vec{q}, \tau) J_{\mathbf{x}}(\vec{q}, 0) \rangle$ ,  $\text{Re}\sigma(\vec{q}, \omega) = -\text{Im}[\Pi_{\mathbf{J}}(\vec{q}, \omega)/\omega]$  which can be evaluated using our Bose field propagators. For  $\delta \rightarrow 0^+$ , the only non vanishing contribution comes from the  $1/N$  corrections given in Fig. 3. In this limit this involves a convolution of boson propagators with an interband fermion bubble. We found

$$\text{Re}\sigma(\vec{q}, \omega) = \frac{\pi t_{pd}^2}{2NN_s} \sum_{\mathbf{p}} (1 - \overline{\gamma_{\vec{k}+\vec{q}-\mathbf{p}}^2}) \left[ \frac{1}{\omega - \Delta - \omega_{\mathbf{p}}^e} \delta(\omega - \Delta - \omega_{\mathbf{p}}^e) + (\omega \rightarrow -\omega) \right]. \quad (43)$$

Clearly, in the insulating limit for  $\delta \rightarrow 0^+$  the exciton mode gives rise to the continuum in the optical spectrum whereas the sound (holon) mode is completely screened out at half filling. The opposite happens for  $\delta \rightarrow 0^-$  and the roles of the holon and the exciton modes are interchanged, but one reconstructs the same incoherent spectrum. The onset of absorption at this order ( $1/N$ ) begins at  $\Delta\mu + \Delta = \lambda_0(\delta = 0^+)$ . At next order  $\mathcal{O}(1/N^2)$ , (not calculated here), we would find the optical gap equals  $\Delta\mu = \lambda_0 - \Delta$ . This is shown in Fig. 4. At finite positive (negative) doping, the screening of the sound (exciton) is no longer complete, because all modes ( $\pm\omega_{\vec{q}}^e$ ,  $\pm\omega_{\vec{q}}^e$ ) start to be present in the boson propagators. Moreover intraband processes have to be taken into account. Eventually absorption develops inside the insulating charge transfer gap.

These are incoherent contributions to the optical conductivity. In addition there will be coherent contributions carrying a spectral weight proportional to  $\delta$  arising from the quasiparticle modes.

Even though  $\omega_{\vec{q}}^e$  ( $\omega_{\vec{q}}^e$ ) is not involved in the current-current correlator in the zero hole doping limit  $\delta = 0^+$ , ( $\delta = 0^-$ ), it is essential for the understanding of the single particle spectral function which appears in the photoemission and inverse photoemission spectrum. The spectral density on the copper site is  $A_{\mathbf{d}}(\omega) = -1/\pi \text{sgn}\omega \text{Im}G_{\mathbf{d}}(\omega)$  where  $G_{\mathbf{d}}(i\omega_n) = \text{FT} \left[ -\langle d_i(\tau) b_i^{\dagger}(\tau) b_i(0) d_i^{\dagger}(0) \rangle \right]$  is the Green function for the physical d-fermions. In the limit  $\delta \rightarrow 0$  the quasiparticle contribution (order  $(1/N^0)$ ) vanishes and  $A_{\mathbf{d}}(\omega)$  is given by the  $1/N$  corrections considered by Sá de Melo and Doniach and Pattnaik and Newns [17]. Near the insulating limit one finds

$$A_{\mathbf{d}}(\omega) = \frac{1}{2NN_s} \sum_{\vec{q}, \alpha} \delta(\omega - \varepsilon_{\mathbf{d}} + \omega_{\vec{q}}^{\alpha}) |Z_{\vec{q}}^{\alpha}| \quad (44)$$



Figure 3: Leading  $1/N$  corrections in the small doping limit to (a) the current-current correlator and (b) the spectral density on copper sites. The solid line indicates the quasiparticle fermion propagator and the dashed line indicates the b-boson propagator.

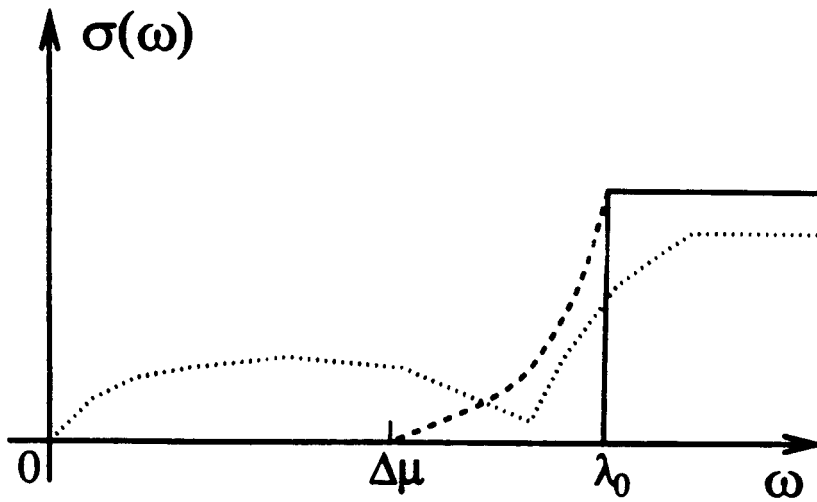


Figure 4: A schematic plot of optical absorption in the insulating limit to order  $1/N$  (solid line). At next order in  $1/N$ , the absorption begins at  $\Delta\mu = |\lambda_0 - \Delta|$  (dashed line). Upon doping, a rapid transfer of optical weight to low energy is expected (dotted line).

$$= -\frac{1}{\pi^2 N_s^2} \sum_{\vec{k}, \vec{q}} \int_{-\infty}^{\infty} d\omega' \text{Im} G_{dd}(\vec{k} + \vec{q}, \omega + \omega') \text{Im} G_b(\vec{q}, \omega') [\theta(-\omega' - \omega) - \theta(-\omega')]$$

with  $G_{dd}(k, \omega) \equiv \langle d_{\vec{k}}(\omega) d_{\vec{k}}^{\dagger}(\omega) \rangle$  and  $G_b(q, \omega) = \langle b_{\vec{q}}^{\dagger}(\omega) b_{\vec{q}}(\omega) \rangle$ .

The momentum summation in (3) spreads out the  $\delta$ -functions giving rise to two broad continuum synonymous to the upper and lower Hubbard bands. Their positions are determined by the arguments of the  $\delta$ -functions which for  $\delta \rightarrow 0^+$ ,  $\Delta \approx 4t_{pd}^2 \overline{\gamma_{\vec{k}}^2} / (\varepsilon_p^0 - \varepsilon_d^0) \ll \lambda_0$ , are given by

$$\varepsilon_d - \omega_{\vec{k}}^e \simeq \varepsilon_d + \Delta \Omega(\vec{k}); \quad \varepsilon_d - \omega_{\vec{k}}^h \simeq \varepsilon_d^0 + \Delta(1 - \Omega(\vec{k})) \quad (45)$$

while for  $\delta \rightarrow 0^-$ ,  $\lambda_0 \approx 4t_{pd}^2 \overline{\gamma_{\vec{k}}^2} / (\varepsilon_p^0 - \varepsilon_d^0) \ll \Delta$

$$\varepsilon_d - \omega_{\vec{q}}^e \simeq \varepsilon_d - \lambda_0 \Omega(\vec{q}); \quad \varepsilon_d - \omega_{\vec{q}}^h \simeq \varepsilon_p^0 - \lambda_0(1 - \Omega(\vec{q})). \quad (46)$$

It is clear now that both modes are essential to construct the spectral function. The spectral density is schematically depicted in fig. 5, which shows that in the  $p-d$  charge transfer system quasiparticle states are introduced at the top of the lower Hubbard band ( $\text{Cu}^{++}$ ) and at the bottom of the upper ( $\text{O}^{--}$ ) Hubbard band for electron and hole doping respectively. This resembles the Mott-Hubbard picture from the energetic point of view. The quasiparticle states which are induced by doping however, are strong coupling limits of the Kondo resonances [8] describing states which have no analog in the insulating state. They form the narrow quasiparticle band  $E_1(k)$  of width  $\sim 8r_0^2 t_{pd}^2 / \Delta$  around the renormalized level  $\varepsilon_d$  with a Luttinger Fermi surface and give rise to the dispersive features observed in angle resolved photoemission. [27] It is clear from Fig. 2 that the closing of the charge transfer gap is equivalent to the softening of the exciton mode at zero  $\vec{q}$ .

To conclude, this lecture, we have shown that the slave boson technique provides a simple picture of the infinite- $U$  and finite charge transfer energy- $E$  aspects of the strong correlation problem. The physics of the metal charge transfer insulator transition as well as the distribution of the single particle spectral density can be understood in terms of collective bosonic excitations which evolve into the physical collective modes in a strongly correlated metal upon doping. The large  $N$  expansion to next to leading order in  $N$ , substantiates and combines the Gutzwiller and the Hubbard pictures.

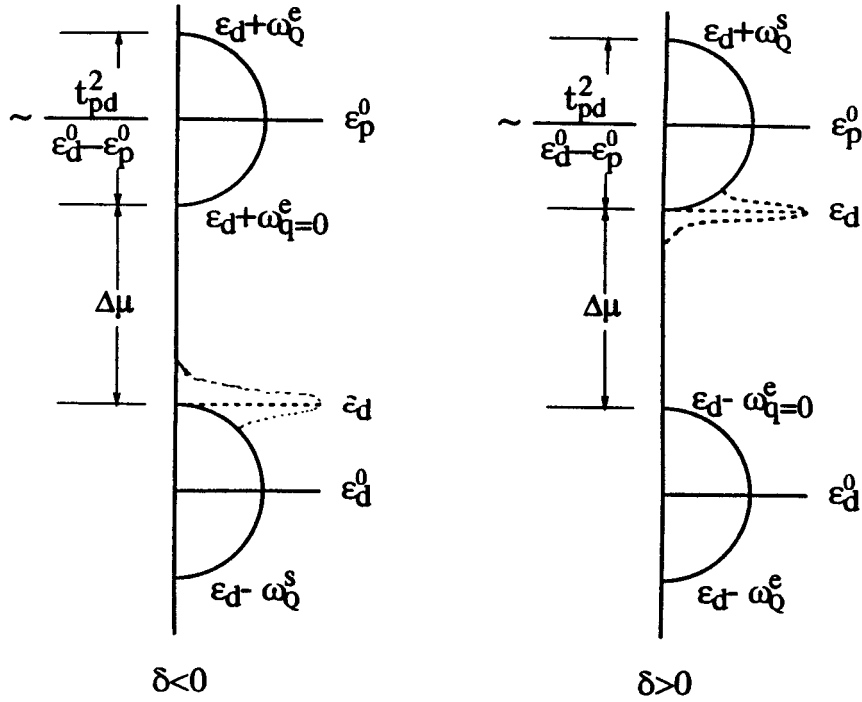


Figure 5: A schematic picture of the single particle spectral density in the two band model in the insulating limit (solid lines) and upon hole doping (dashed line). The bare and renormalized energy scales are indicated and  $\Delta\mu = \omega_{q=0}^e = |\lambda_0 - \Delta|$ . The width of the continuum is determined by the dispersion for the modes at the zone boundary  $Q = (\pi, \pi)$ .

## 4 Heavy Fermions and High $T_c$ superconductors

In this lecture we will analyze the effects of the conduction electron (p electrons) bandwidth. This analysis is important to establish a connection with the heavy fermion systems. [7] [6].

In these systems the conduction electron band is very broad, (typically several electron volts) and the kinetic energy of these carriers is the largest energy scale in this problem. The low energy excitations in this system, are resonances embedded in the continuum of the conduction band. These excitations are the lattice version of the weak coupling Kondo resonances described in section 2. It is instructive to contrast the heavy fermion limit with the  $t_p = 0$  limit discussed in the previous section. The latter situation, bears some similarity with the strong coupling limit of the Kondo problem discussed in the second section.[11]

To simplify the algebra we will study a simplified oxygen dispersion defined by replacing  $\epsilon_p$  by  $\epsilon_p^o + 2t_p - 2t_p(\sin^2 \frac{k_x}{2} + \sin^2 \frac{k_y}{2}) \equiv \epsilon_p(k)$ .

While this corresponds to a very special form of the oxygen overlap it captures the essential physics of the crossover between the heavy fermion regime and the small  $t_p$  regime discussed in the previous section. [8]. The mean field equations can be expressed in terms of  $\rho(y) \equiv \sum_K \delta(y - \frac{\gamma_K^2}{2})$ ,  $\gamma_K \equiv \sqrt{\sin^2 \frac{K_x}{2} + \sin^2 \frac{K_y}{2}}$  as:

$$\epsilon_d - \epsilon_d^o = \int_{y_F}^1 \frac{dy \rho(y)}{R(y)} 8t_{pd}^2 \quad (47)$$

$$\frac{1}{2} - r_o^2 = \int_{y_F}^1 dy \rho(y) \frac{1}{2} \left[ 1 + \frac{(\epsilon_p - 4t_p y + 2t_p - \epsilon_d)}{R(y)} \right] \quad (48)$$

$$(49)$$

$y_F$  is simply related to the Fermi wave vector which determines the total number of particles according to Luttinger theorem  $\int_{y_F}^1 \rho(y) dy = \frac{1+\delta}{2}$ .

To make progress analytically it is convenient to make the "spherical band approximation"  $\rho(y) \simeq 1$ , which allows to write explicitly the non-linear mean field equations:

$$\frac{1}{4} - \frac{\delta}{4} - r_o^2 = \frac{1}{8t_p} [R(y_F) - R(1)] + \frac{r_o^2 t_{pd}^2}{8t_p^2} R_1 \quad (50)$$

$$\epsilon_d - \epsilon_d^o = \frac{t_{pd}^2}{2t_p^2} [R(1) - R(y_F)] + \left[ (\epsilon_p^o + 2t_p - \epsilon_d) - \frac{r_o^2 t_{pd}^2}{t_p} \right] R_1 \quad (51)$$

$$(52)$$

In this approximation  $1 - y_F = \frac{1+\delta}{2}$  and we defined:

$$R_1 = \log \left[ \frac{8t_p(R(1) - (\epsilon_p - 2t_p - \epsilon_d)) + 8r_o^2 t_{pd}^2}{8t_p(R(y_F) - (\epsilon_p + 2t_p - 4y_F t_p - \epsilon_d)) + 8r_o^2 t_{pd}^2} \right] \quad (53)$$

$R(y) \equiv \sqrt{(\epsilon_p^o + 2t_p - \epsilon_d - 4t_p y)^2 + 8r_o^2 t_{pd}^2 y}$  has the same meaning as in the previous section.

It is convenient to combine the two equations (50) and (51) into

$$\epsilon_d - \epsilon_d^o = \frac{4t_{pd}^2}{t_p} \left[ r_o^2 + \frac{\delta}{4} - \frac{1}{4} \right] + \frac{t_{pd}^2}{2t_p^2} (\epsilon_p^o + 2t_p - \epsilon_d) R_1 \quad (54)$$

There are several characteristic energies which can be very low:  $8r_o^2 t_{pd}^2$  is the hybridization energy and  $\epsilon_p - \epsilon_d - 2t_p \equiv Eg$  is the distance from the renormalized level to the bottom of the  $p$  band.  $Eg^B = \epsilon_p - 2t_p - \epsilon_d^o$  is the distance between the bare and  $d$  level and the bottom of the  $p$  band.

We study the limit  $t_p \gg \frac{t_{pd}^2}{Eg^B}$ , and begin with the limit of a *very small* number of holes. In this limit we will show that the two low energy scales obey the following inequality

$$4r_o t_{pd} \ll Eg \quad (55)$$

which will guide our analysis. When (55) is satisfied it is legitimate to expand eq. (50) in powers of  $r_o^2$  to first order. Neglecting factors of  $\delta$  whenever possible we obtain

$$R_1 \simeq \log \left[ \frac{(Eg + 4t_p)(Eg + 2t_p)}{Eg(Eg + 6t_p)} \right] \quad (56)$$

and

$$-\frac{\delta}{2} - r_o^2 = \frac{r_o^2 t_{pd}^2}{2t_p} \left\{ \frac{1}{2(\epsilon_p^o - \epsilon_d)} - \frac{1}{Eg} \right\} + \frac{r_o^2 t_{pd}^2}{8t_p^2} \log \frac{(Eg + 2t_p)(Eg + 4t_p)}{Eg(Eg + 6t_p)} \quad (57)$$

This equation determines the proportionality between  $r_o^2$  and  $\delta$  once  $\epsilon_d$  (and therefore  $Eg$ ) are determined. To determine  $Eg$  we use the second mean field equation (Eq. 54). Since Assuming (55) and  $t_{pd}^2 \ll E_g^B t_p$ ,  $\frac{t_{pd}}{t_p} \ll 1$  we see that  $R_1$  must be large, i.e.  $Eg \sim 0$  in order to satisfy eq. (54):

$$Eg \simeq \frac{4t_p}{3} e^{-\frac{t_p E_g^B}{2t_{pd}^2}} \quad (58)$$

Physically this equation means that the renormalized  $d$  level is exponentially close to the bottom of the  $p$  band. We can now go back to eq. (57) to solve for  $r_o^2$ . In this limit

$$r_o^2 \simeq \delta \frac{t_p Eg}{t_{pd}^2} \simeq \frac{4}{3} \delta \frac{t_p^2}{t_{pd}^2} e^{-\frac{t_p E_g^B}{2t_{pd}^2}} \quad (59)$$

Now we can verify that the inequality  $8r_o^2 t_{pd}^2 \sim 8\delta t_p Eg \ll E_g^2$  which we assumed in our analysis, is indeed satisfied provided that  $\delta \ll \delta_c = \frac{E_g}{8t_p} = \frac{1}{16} \exp - \frac{t_p E_g^B}{2t_{pd}^2}$ .

When  $\delta$  increases the  $d$  level moves inside the  $p$  band. The large  $N$  version of the Zhang Rice singlet of the previous section turns into the large  $N$  version of the Kondo resonance as we leave the regime  $\delta \ll \delta_c$  to enter the heavy fermion regime  $\delta > \delta_c$ . In the heavy fermion regime the  $d$  level is deep inside the  $p$  band,  $Eg$  is negative and large and the two small energy scales are  $|\epsilon_p - \epsilon_d + 2t_p(1 - 2y_F)| \ll 8r_o^2 t_{pd}$ . The analysis of the mean field equations is now simpler. Using the fact that  $r_o^2$  is very small we insert  $R(y_F) \simeq \epsilon_p(y_F) - \epsilon_d > 0$  and  $R(1) = \epsilon_d - \epsilon_p(1)$  in eq. (50)) and determine

$$\epsilon_d = \epsilon_p(1) - 2t_p(1 - \delta) \quad (60)$$

The physical interpretation of this result is that the location of the  $d$  level is approximately the position of the Fermi level of a gas of  $\delta$  oxygen holes.

We then determine the value of  $r_o^2$  from eq. (57). Assuming again that  $r_o^2$  will be small, we substitute  $R(1) - (\epsilon_p^o - 2t_p - \epsilon_d) \simeq 4t_p\delta$ ,  $R_1 = \log(\frac{4t_p^2\delta}{3r_o^2 t_{pd}^2})$  in (57) and solve for  $r_o^2$ .

$$r_o^2 = \frac{4}{3} t_p^2 \frac{\delta}{t_{pd}^2} \exp - \frac{t_p(E_g^B + 2t_p\delta)}{t_{pd}^2(2 - \delta)} \quad (61)$$

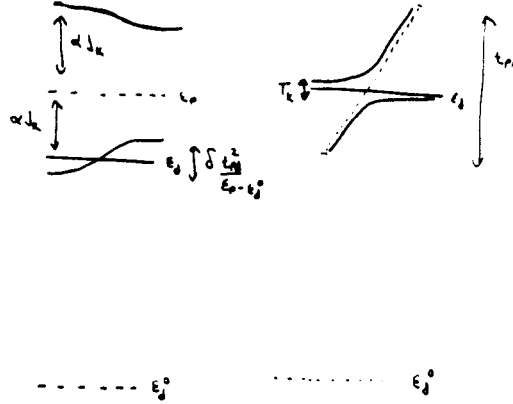


Figure 6: Bare (dotted lines) and renormalized (solid lines) band structure of the Anderson lattice in the regime corresponding to the copper oxides (left), and the regime corresponding to the heavy fermions (right).

which is indeed exponentially small when  $t_p > t_{pd}$ . Furthermore it decreases exponentially as  $\delta$  increases. We illustrate the renormalized band structure characteristic of the  $t_p \gg \frac{t_{pd}^2}{E_g^B}, \delta > \delta_c$  regime in Fig. 6

It is instructive to use the analysis of this and of the previous section to understand how the copper oxides (HTS) and the heavy fermion (HF) systems, which are both described by the Anderson lattice hamiltonian have very different low energy properties.

There are essential differences between the heavy fermions and the high temperature superconductors. In the heavy fermions the doping is large and  $t_{pp} \gg J_K$ , where  $J_K \approx t_{pd}^2/E_g^B$ . The high  $T_c$  materials are closer to the opposite limit  $t_{pp} < J_K$ . In the heavy fermion materials the magnetic interaction between the moments is comparable with the Kondo temperature,  $J \leq T_{coh}$ , as a result the heavy fermions obey Curie law above the coherence temperature. The opposite behavior occurs in the high  $T_c$  materials, the coherence temperature is much smaller than the exchange, and the susceptibility is Pauli like. There are no free magnetic moments above  $T_{coh}$ , in this case Heavy fermion masses, are the result of the free moment entropy which is transferred to the Fermi liquid below the coherence temperature. In the heavy Fermion systems  $\log 2 \simeq \gamma T_{coh}$  so  $\gamma$  scales as  $\frac{1}{T_{coh}}$  while in the HTS materials the spin entropy is quenched at a scale  $J$  and  $\gamma \sim \frac{1}{J}$ . In the HTS, there is never a free moment as long as  $T \leq J$  and the mass renormalizations

Materials:	Copper Oxides	Heavy Fermions
Similarities: in both electrons form a	system local moments Luttinger fermi surface	and conduction contains $1 + \delta$ holes
Energy scales	$J \gg T_{coh}$ $t_p \leq J_K$	$J \leq T_{coh}$ $t_p \gg J_K$
	$\epsilon_p - \epsilon_d \geq t_{pd}$	$\epsilon_p - \epsilon_d \gg t_{pd}$
Susceptibility	$\chi \approx const$	$\chi \approx \frac{1}{T} T \gg T_{coh}$
Binding Energy	$\frac{t_{pd}^2}{\epsilon_p - \epsilon_d}$	$T_K \simeq \frac{t_{pd}^2}{t_{pd}} e^{-\frac{2t_{pd}(\epsilon_p - \epsilon_d)}{t_{pd}^2}}$
Coherence temperature	$T_{coh} < \delta \frac{t_{pd}^2}{(\epsilon_p - \epsilon_d)}$	$T_{coh} \simeq T_K$
Superfluid analogy	pairs Bose condense	BCS limit

Table 3: High  $T_c$  Superconductors and Heavy Fermions: Differences and Similarities

are not large.

The physics above the coherence temperature is very different in the two materials. In the heavy fermion systems the scale of the coherence temperature is set by the Kondo temperature. This is the binding energy of the spin to the conduction electron compensation cloud that forms the Kondo resonance. It is defined as the difference between the energy with  $r_0 \neq 0$  and the energy with  $r_0$  set equal to zero. For  $t_{pd} \ll E_g^B$  it is given by  $\frac{(t_{pd})^2}{E_g^B}$ , which is the delocalization energy. The formula for the binding energy is reminiscent of the transition temperature of a BCS superconductor.

In the HTS limit the binding energy of the singlet is of the order of  $J_K$ , much larger than the coherence temperature which is only a fraction of  $\delta J_K$ . In the superfluid analogy, the ZR limit is close to the Bose condensation of tightly bound pairs of molecules in which the condensation temperature is determined by the excitations of collective modes and is much smaller than the binding energy. In the regime  $T_{coh} \ll T \ll J$  the transport is dominated by incoherent holes but the spins are locked by the superexchange interaction and the susceptibility is weakly temperature dependent. This discussion is summarized in table 3.

## 5 The valence and the charge transfer instabilities

The large  $N$  expansion gives us an approximate realization of how one goes about constructing a low energy hamiltonian. It allows us to examine how varying the high energy parameters affects the properties of the quasiparticle (saddle point) hamiltonian and the effective interactions among the quasiparticles. In this lecture we continue our investigation of the infinite  $U_d$  extended Hubbard model and study the effects of the nearest neighbor copper oxygen repulsion  $V$  in the hamiltonian (18).

We show that when this term is large enough it gives rise to a qualitative new features: a) The coexistence of two valences in a region of parameter space. We call the critical point where this phenomena first occurs the Valence Instability (VI) point. Mathematically the two valences appear as two different solutions of the mean field equations describing different copper-oxygen content. b) The valence instability is a transition that takes place at *fixed doping* as we vary the interaction  $V$ . As we vary the doping the two mean field solutions exchange stability and this gives rise to a region of negative curvature in the energy vs. doping plot. The point where the compressibility and the charge transfer susceptibility calculated at fixed chemical potential, diverge defines the charge transfer instability (CTI) point. c) Before the compressibility turns negative phase separation takes place. Near the phase separation region superconductivity results. [16] These conclusions agree qualitatively with the weak coupling (small  $U_d$ ) investigations of the same model which are the subject of P. Littlewood in this school. The quantitative differences between the large and the small  $U$  limits of this model have been discussed recently. [35] c) The nearest neighbor repulsion gives us another knob which we can use to tune the metal charge transfer insulator transition. In the previous sections we found that the transition can be viewed as the disappearance of the Kondo resonance (vanishing of  $r_0$  in the  $N = \infty$  limit), or as the collapse of the Mott Hubbard gap (the vanishing of  $\omega_{exciton}$ ). [41]. When  $V$  is small or zero, the two effects occur at the same point. One is left, however, with the feeling that the two phenomena are not necessarily related, and do not need to take place at the same point. The disappearance of the Kondo occurs at the  $N = \infty$  level, while the collapse of the charge transfer gap is seen in the incoherent part of the spectra which

appears at the next to leading  $\frac{1}{N}$  order. For sufficiently large values of  $V$ , we can separate the two effects. The metal insulator transition becomes first order, and the quasiparticle residue jumps. The vanishing of the exciton energy takes place *at the VI point* which now occurs at finite doping. [35]

Our starting point is the Hamiltonian (18), which we treat with the functional integral methods of the previous section. We treat the  $V_2 = 0$  and  $J = 0$  case which requires the introduction of two scalar Hubbard Stratonovich fields,  $X$  and  $Y$ . The more general case is discussed in ref. [35]. In terms of these fields the partition function is given by:

$$Z = \int Dp_{\alpha\sigma}^\dagger Dp_{\alpha\sigma} Dd_{\sigma}^\dagger Dd_{\sigma} Db^\dagger Db D\lambda DX DY e^{-\int_0^\beta S d\tau}, \quad (62)$$

$$S = \sum_i \left[ \sum_{\sigma} d_{i\sigma}^\dagger \frac{\partial d_{i\sigma}}{\partial \tau} + \sum_{\sigma\alpha=\pm x, \pm y} p_{i\sigma\alpha}^\dagger \frac{\partial p_{i\sigma\alpha}}{\partial \tau} + b_i^\dagger \frac{\partial b_i}{\partial \tau} \right] + \sum_i \left[ i\lambda_i \left( b_i^\dagger b_i - \frac{N}{2} \right) + \frac{N}{2V} (X_i^2 + Y_i^2) \right] + H, \quad (63)$$

$$H = \sum_{i,\sigma} d_{i\sigma}^\dagger d_{i\sigma} (\varepsilon_d^0 + i\lambda_i + X_i + iY_i) \quad (64)$$

$$- \frac{1}{2} \sum_{i,\sigma,\alpha=\pm x, \pm y} p_{i\sigma\alpha}^\dagger p_{i\sigma\alpha} (X_i - iY_i) + \varepsilon_p^0 \sum_{i,\sigma,\alpha=\pm x, \pm y} p_{i\sigma\alpha}^\dagger p_{i\sigma\alpha} - \frac{t_{pd}}{\sqrt{N}} \sum_{i,\sigma} \left[ \left( p_{i\sigma x}^\dagger - p_{i\sigma-x}^\dagger + p_{i\sigma y}^\dagger - p_{i\sigma-y}^\dagger \right) d_{i\sigma} b_i^\dagger + c.c. \right] \quad (65)$$

In the large  $N$  limit the partition function is controlled by the saddle point. The bosonic fields are uniform time-independent numbers  $\langle b_i \rangle = b_0 = \sqrt{N}r_0$ ,  $\langle \lambda_i \rangle = -i\lambda_0$ ,  $\langle X_i \rangle = X_0$  and  $\langle Y_i \rangle = -iY_0$ . Notice that the paths for  $\lambda_i$  and  $Y_i$  in the functional integral have been deformed from the real axis inside the complex plane to meet the saddle point solutions. At this point the model has become a tight-binding model for free fermions describing the coherent motion of the quasiparticles of a Fermi liquid. The only effect of the interactions is in the renormalization of the tight-binding parameters:  $r_0$  multiplicatively renormalizes the hopping  $t_{pd}$  leading to a reduction of the quasiparticle bandwidth, whereas  $\lambda_0$ ,  $X_0$  and  $Y_0$  shift the bare atomic levels

$$\varepsilon_p = \varepsilon_p^0 - (X_0 - Y_0)$$

$$\varepsilon_d = \varepsilon_d^0 + (X_0 + Y_0) + \lambda_0$$

The mean field equations are a generalization of the ones written in the previous sections, with  $t_p = 0$  :

$$\lambda_0 = \frac{1}{N_s} \sum_k \frac{4t_{pd}^2 \gamma_k^2}{R_k} (f_{1k} - f_{2k}) \quad (66)$$

$$\frac{1}{2} = r_0^2 + \frac{1}{N_s} \sum_k (u_k^2 f_{1k} + v_k^2 f_{2k}) \quad (67)$$

$$X_0 - Y_0 = -2Vn_d = -\frac{2V}{N_s} \sum_k (u_k^2 f_{1k} + v_k^2 f_{2k}) \quad (68)$$

$$X_0 + Y_0 = 2Vn_p = \frac{2V}{N_s} \sum_k (v_k^2 f_{1k} + u_k^2 f_{2k} + f_{3k}) \quad (69)$$

$$\frac{(1+\delta)}{2} = \frac{1}{N_s} \sum_k (f_{1k} + f_{2k} + f_{3k}) \quad (70)$$

where  $u_k^2 \equiv \frac{1}{2} \left(1 + \frac{\varepsilon_p - \varepsilon_d}{R_k}\right)$ ,  $v_k^2 \equiv \frac{1}{2} \left(1 - \frac{\varepsilon_p - \varepsilon_d}{R_k}\right)$  with  $R_k^2 \equiv (\varepsilon_p - \varepsilon_d)^2 + 16t_{pd}^2 r_0^2 \gamma_k^2$ , and  $f_{ik} \equiv f(E_i(k) - \mu)$ . The  $E_{ek}$  represent the quasiparticle energies and are still given by eq. (26) with  $\varepsilon_p^0$  replaced by  $\varepsilon_p$ .

The mean field equations can be manipulated into a form that resembles the mean field equations of an ising magnet provided that we identify the magnetization with  $n_p - n_d$  and the external field with the difference in energy of the Hartree Fock levels, [30] with  $n_p \equiv \sum_{\sigma\alpha=s,y} p_{i\sigma\alpha}^+ p_{i\sigma\alpha}$ .

This quantity can be rewritten by exploiting the constraint and the total particle number condition Eqs. (67) and (70)

$$n_p - n_d = -\frac{1}{2} (1 - \delta - 4r_0^2)$$

Then, defining the Hartree gap

$$\Delta_H \equiv \varepsilon_p^0 - \varepsilon_d^0 + 2V(n_d - n_p)$$

the above expression represents a straight line in the  $\Delta_H - r_0^2$  plane,

$$r_0^2 = -\frac{1}{4V} \Delta_H + \frac{1}{4V} [\Delta_0 + Vq(1 - \delta)] \quad (71)$$

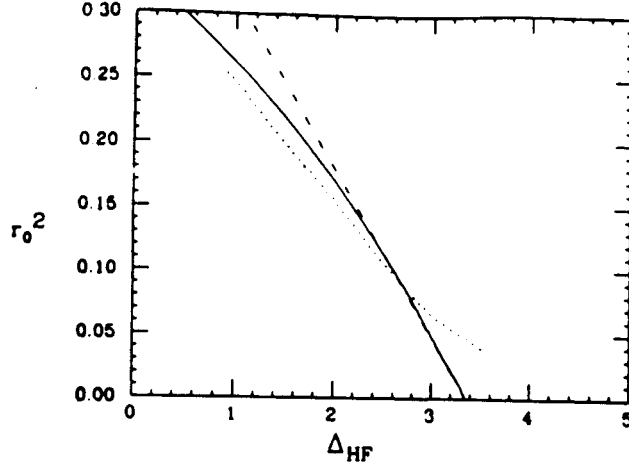


Figure 7:  $r_0^2$  vs  $\Delta_H$  for doping  $\delta = 0$  and  $\delta = 0.2$ . The straight line is given by Eq. 69 in the text defining the critical slope at which the mean field equations cease to have a unique solution at zero doping. All energies in units of  $t_{pd}$

with  $\Delta_0 \equiv \varepsilon_p^0 - \varepsilon_d^0$ .

The self-consistency problem is then solved by finding the intersection(s) of the straight line Eq.(71) with the curve  $r_0^2 = r_0^2(\Delta_H, \delta)$  obtained by solving Eqs. (66) and (67) together with the condition (70) for all the values of  $\Delta_H$ . We show  $r_0^2(\Delta_H)$  in Fig.7 at doping  $\delta = 0$  and  $\delta = 0.2$  together with the straight line at zero doping.

The curve  $r_0^2 = r_0^2(\Delta_H, \delta)$  does not depend on  $V$ : the same curve would be obtained in the three band Hubbard model (without  $V$ ) [4] by simply varying the bare CT gap  $\Delta_0$ . On the other hand the coefficient of the straight line (71) is  $1/(4V)$  so that the number of intersections depends on  $V$ . Then a critical value  $V^*(\delta)$  exists such that, for  $V < V^*(\delta)$ , the straight line is too steep and only intersects once the curve  $r_0^2 = r_0^2(\Delta_H, \delta)$ . If  $V > V^*(\delta)$ , instead, three solutions occur corresponding to one maximum and two minima in the free energy functional. In particular, in the case with  $t_{pp} = 0$ ,  $\delta = 0$ ,  $V^* \approx 1.76t_{pd}$ .

When  $V > V^*(\delta)$ , with increasing doping, the mean field solution presents a first order valence transition from a d-like metal with a small  $r_0^2$  to a more p-like metal with a larger  $r_0^2$ , (having larger oxygen content).

The MCTI transition is affected by the presence of the valence transition:

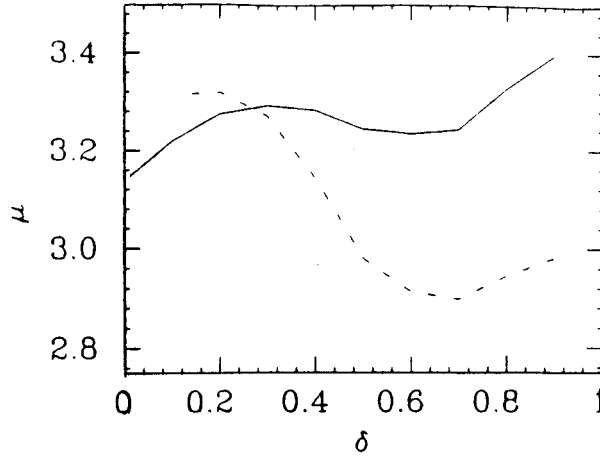


Figure 8: Chemical potential as a function of doping for  $t_{pp} = 0.2t_{pd}$ ,  $U_p = 0$  and  $V = 2.3t_{pd}$  for  $\Delta_0 = 2.2t_{pd}$  (continuous line) and  $\Delta_0 = 2.4t_{pd}$  (chain-dotted line).

while the MCTI transition is second order when  $V < V^*$ , it becomes of the first order when  $V > V^*$ . In this latter case the valence transition line in the plane  $\Delta_0 - \delta$  starts from the MCTI transition point.

Notice that the mean field Eqs.(66)-(70) describe the system at fixed doping, in the absence of homogeneous density fluctuations. Then the fact that the mean field equations exhibit a valence change varying the doping is indicative that allowing density fluctuations can result in phase separation between d-like and p-like phases. This occurrence can be investigated in the grand canonical ensemble by studying the density-density correlation functions at fixed chemical potential. We also compute the chemical potential as a function of doping from the mean field equation. A typical case is shown in Fig.8, where it is apparent that the chemical potential is not a monotonically increasing function of the number of particles. In particular there are points where the inverse compressibility  $\chi^{-1} \equiv \frac{d\mu}{dn}$  is zero. A diverging compressibility is a signature of phase separation requiring the use of a standard Maxwell construction to determine the stable region in the phase diagram. It is important to realize that, when the compressibility diverges (that is the static total density fluctuations diverge), also the static CT susceptibility  $\chi_{CT}$  diverges because the total density and the CT modes are coupled[16] and therefore

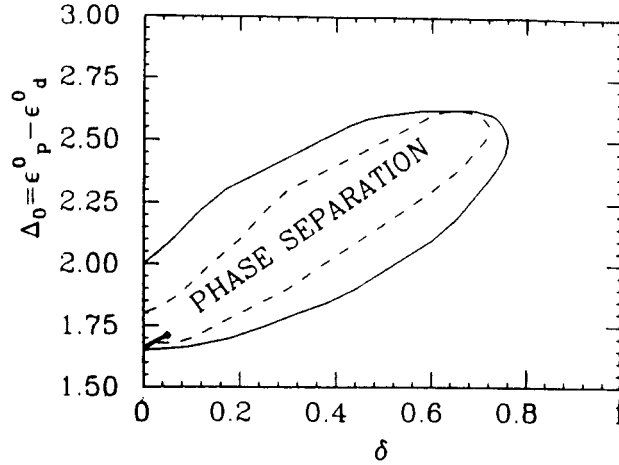


Figure 9: Phase diagram  $\Delta_0/t_{pd}$  vs  $\delta$  for  $t_p = 0.2t_{pd}$ , and  $V = 2.3t_{pd} > V^*$ . To obtain a more realistic phase diagram an oxygen oxygen repulsion term  $U_p = 2.0t_{pd}$  was added to the Hamiltonian. The first order p-d valence transition is shown by a thick line ending at a critical point indicated by the diamond. The metal-CT insulator transition is first order and occurs at the crossing point between the vertical axis and valence transition line. From reference 34. The dashed line indicates the points where the compressibility diverges. The solid line encloses the phase separation region, as determined from a Maxwell construction.

the unstable eigenmode cause all the elements of the susceptibility matrix to diverge. This is intuitively seen by noting that a decoupled CT mode means that the intracell charge fluctuates from copper to the surrounding oxygens and vice versa with  $\delta n_{d_i} + \delta n_{p_i} = 0$ . On the other hand the Hubbard repulsion depresses the charge fluctuations on copper, which have to satisfy a constraint. This strongly favors a CT mode accompanied by a total intracell charge fluctuation  $\delta n_{d_i} + \delta n_{p_i} \neq 0$  because copper cannot always accept all the charge that oxygen can provide. A large N phase diagram for a typical set of parameters is shown in Fig. 9, where the dashed line indicates the points where the compressibility and the CT susceptibility become infinite. Fig (9) shows a first order transition line ending with a critical point (indicated by a dot). By increasing  $V > V^*$  this transition line becomes longer and the critical point moves away from the MCTI transition point deeper and deeper

inside the unstable region. Even though the critical point lays inside the physically unaccessible region of negative compressibility, it is nevertheless instructive to notice that this point is reminiscent of the MCTI transition point at  $V < V^*$ . In fact, not only the critical point continuously evolves from the MCTI point when  $V$  exceeds  $V^*$ , but also at both the MCTI point when  $V < V^*$  and at the critical point when  $V > V^*$ , the compressibility goes to zero. In both cases the excitonic mode becomes soft and the zero momentum dynamical scattering amplitude  $\Gamma_\omega$  diverges. Notice, however, that away from half filling  $r_0$  is not critical.

In ref [16] an analysis of the effective interactions between the quasiparticles was carried out. Near the phase separation region it showed that the normal phase is unstable against an  $s$  wave superconducting phase. Therefore in this model phase separation, the charge transfer instability and superconductivity are closely related phenomena.

## 6 Conclusions

In these lectures I have tried to give the student a feeling for the slave boson technique and the large  $N$  expansion in the strong correlation problem. It is clear that the formalism gives a good starting point for treating the itinerant and the localized aspects of the strong correlation problem. Several extensions of the auxiliary boson formalism presented here, that go beyond the strict  $1/N$  framework, may prove to be necessary, to approximate better the physics at  $N = 2$ .

One is the possibility of expanding around states where the slave bosons are not condensed. For a guide to this rapidly developing field see refs [32] [24] [25] Another possibility is to consider instanton solutions, when the mean field equations have two nearly degenerate minima. It may be necessary to consider some tunneling between the different mean field solutions describing the positive and negative doping, near the Mott transition. It is certainly important for a proper understanding of the physics of the charge transfer instability.

We have emphasized that the collective modes, described by the Bose fields, play an important role in all physical quantities. To describe the  $SU(2)$  situation, we may want to use the four boson approach [33], which incorporates the spin degrees of freedom very naturally. Some important

technical advances have recently taken place. [34]. It would be interesting to extend the insights gained from the systematic use of the large  $N$  method to this more realistic context.

A lot is to be gained from comparing the results of the large  $N$  expansion in finite dimension with the solution of the same models in  $d = \infty$  for  $N = 2$ . [37] A common link between the two tools is the extensive use of impurity models. The results of the large  $N$  expansion carried out to next to leading order in  $\frac{1}{N}$  agree qualitatively with the exact solutions in large dimensionality obtained via mappings onto impurity problems. Furthermore they give a clue as to how the  $\frac{1}{d}$  expansion will resolve the degeneracies of the  $d = \infty$  solution. On the other hand the large  $d$  solution contains both the quasiparticle features and the incoherent features in the leading order. Therefore it offers a very simple treatment of the finite temperature aspects of the strong correlation problem. Here, the large  $d$  approach will provide a clue as to the correct interpretation of the large  $N$  expansion at *finite temperature*. An important, and poorly understood subject.

**Acknowledgment** The material presented in sections 3 and 5 are the result of a recent joint work with Y. Bang C. Castellani M. Grilli R. Raimondi and Z. Wang . I would like to thank them for a fruitful collaboration. M. Rozenberg carefully read this manuscript and made substantial improvements on the original version.

## References

- [1] N. Read and S. Sachdev PRL 66, 1773 (1991) and Int J Mod Phys B5, 219 (1991). J Ye and S. Sachdev PRB44 , 10173 (1991).
- [2] N. Read and D. Newns J Phys. C 16, 3273 (1983). N. Read, *J. Phys. C* **18**, 2651 (1985).
- [3] P. Coleman PRB29, 3035 (1984) PRB 35, 5072 (1987).
- [4] G. Kotliar, P. A. Lee, and N. Read, Physica C 153-155, 538 (1988).
- [5] C. Castellani G. Kotliar R. Raimondi M. Grilli Z. Wang and M Rozenberg, Phys. Rev. Letters, 69, 2009 (1992).
- [6] A. Auerbach and K. Levin, Phys. Rev. Lett. 57, 877 (1986).

- [7] A. Millis and P. A. Lee *Phys. Rev. B* 35, 3394 (1987).
- [8] M. Grilli, G. Kotliar and A. Millis *Phys. Rev. B* 42, 329 (1990).
- [9] S. Barnes *J. Phys. F* 6, 1375 (1976)
- [10] P. Nozieres *J. Low Temp. Phys.* 17, 31 (1974)
- [11] V. Dobrosavljevic and G. Kotliar *Phys. Rev. B* 46, 5366 (1992).
- [12] A. Houghton, N. Read and H. Won *Phys. Rev. B* 35, 5123 (1987).
- [13] B. Jones *Physica B* 171, 53 (1991).
- [14] C. M. Varma, S. Schmitt-Rink, and E. Abrahams, *Solid State Comm.* 62, 681 (1987).
- [15] M.S. Hyberstsen, M. Schlüter, and N.E. Christensen, *Phys. Rev. B* 39, 9028 (1989).
- [16] M. Grilli, R. Raimondi, C. Castellani, C. Di Castro, and G. Kotliar, *Phys. Rev. Lett.* 67, 259 (1991).
- [17] C. A. R. Sá de Melo and S. Doniach, *Phys. Rev. B* 41, 6633, (1990). P.C. Pattnaik and D.M. Newns, *Phys. Rev. B* 41, 880 (1990).
- [18] J. H. Kim, K. Levin and A. Auerbach, *Phys. Rev. B* 39 (1989).
- [19] G. Kotliar, *International Journal of Modern Physics B* Vol. 5, bf 1, 2 341 (1991).
- [20] P.W. Anderson and Z. Zou, *Phys. Rev. Lett.* 60, 132 (1988). 66, 2258 (1991). 1240 (1973).
- [21] M. Grilli, Castellani and G. Kotliar *Phys. Rev. B* 43, 8000 (1991).
- [22] G. Kotliar, *Int. Journal of Mod. Phys. B*, Vol. 1, No. 5 (1988) 711.
- [23] Notice the differences and similarities with the Zhang Rice construction. F.C. Zhang and T.M. Rice, *Phys. Rev. B* 37, 3759 (1988).

- [24] N. Nagaosa and P.A. Lee, *Phys. Rev. Lett* **64**, 2450 (1990). P.A. Lee, *Phys. Rev. Lett.* **63**, 680 (1989).
- [25] L.B. Ioffe and G. Kotliar, *Phys. Rev. B* **42**, 10348 (1990).
- [26] J. Hubbard, *Proc. R. Soc. London Ser. A* **276**, 238 (1963); **277**, 237 (1964); **281**, 401 (1964); **285**, 542 (1965); **296**, 82 (1967).
- [27] . C. G. Olson et. al *Phys Rev B* **42** (1990) 381.
- [28] W. Brinkman and T.M. Rice, *Phys. Rev. B* **2**, 4302 (1970).
- [29] M. Grilli, R. Raimondi, C. Castellani, C. Di Castro, and G. Kotliar, *International Journal of Modern Physics B* Vol . 5, 309 (1991).
- [30] Y. Bang C. Castellani M Grilli and R Raimondi *Phys. Rev. B* **43**, 13724 (1991).
- [31] P.W. Anderson, *Science* **235**, 1196 (1987).
- [32] L.B. Ioffe and A.I. Larkin, *Phys. Rev. B* **39**, 8988 (1990).
- [33] G. Kotliar and A. Ruckenstein. *Phys. Rev. Lett.* **57**, 1362 (1986).
- [34] P. Wolfe P Hirschfeld Rotational invariance. T. Li, P. Wolfe, P. Hirschfeld, *Phys. Rev. B* **40**, 6817 (1989). R. Fresand and P. Wolfe, *Int. Jour. Mod. Phys. B* **6**, (1992), 685 erratum *Int. Journ. Mod. Phys. B* **6**, 3087 (1992). M. Lavagna *Phys. rev. B* **41** 142 (1990) M. Arrigoni and G. Strinati (unpublished). T. Jolicoeur and J C Le Guillou, *Phys. Rev. B* **44** , 2404 (1991) 11413 (1989).
- [35] Y. Bang et. al , R. Raimondi et. al. to appear in *Phys. Rev. B*.
- [36] See lectures by D. Vollhardt in this school.
- [37] A. Georges and G. Kotliar *Phys. Rev. B. Q. Si Int. Jour. Mod. Phys.* 1992. 324.
- [38] M. Grilli and G. Kotliar, *Phys. Rev. Lett* **64**, 1170 (1990).
- [39] see also the lectures of G. Kotliar in the 1991 Les Houches summer school on strongly correlated electrons.

- [40] Z. Wang, Y. Bang, and G. Kotliar, Phys. Rev. Lett. 67, 2733 (1991)
- [41] C. Castellani G Kotliar R Raimondi Z Wang and M. Rozenberg Phys. Rev. Lett. 69, 2009 (1992).